JOURNAL OF PROPULSION AND POWER
Vol. 16, No. 3, May–June 2000

Scarfing and Scalloping Effects on Lobed Forced Mixer at Low-Speed Conditions

S. C. M. Yu,* Y. Hou,† and W. K. Chan*
Nanyang Technological University, Singapore 639798, Republic of Singapore

This paper presents the findings on two aspects of geometric modification to a lobed forced mixer, namely scarfing and scalloping. Scarfing the lobes was achieved by alternately extending and cutting back the lobes at the trailing edge, and scalloping the lobes was achieved by removing a certain percentage of the straight sidewall area in the penetration region. Both modifications were intended to enhance the strength of streamwise circulation without causing any undesirable consequences, such as flow separation at the lobe troughs. Tests were conducted over a range of low-speed subsonic flow conditions (maximum Mach number of ~ 0.07) by using a three-hole pressure probe and a laser Doppler anemometer. The results showed that scarfing the lobes would be more beneficial than scalloping the lobes if the same level of enhancement for the streamwise circulation were to be achieved. Furthermore, for lobes at the same penetration angle and at the same percentage of surface area change, streamwise circulation generated at the trailing edge was actually higher (~ 15%) for the scarfed lobes than for the scalloped lobes. However, the associated mixing and boundary-layer losses incurred by the scarfed lobes would be higher than those of the scalloped lobes. Finally, the combined effects of the two modifications on a lobed mixer, that is, a scarfed and scalloped mixer, however, did not promote any significant streamwise-circulation enhancement.

Nomenclature

A_{wake}	= area bounded by the wake
C_{Ideal}	= normalized streamwise circulation, Ref. 5
C_1	= normalized streamwise circulation, $I_s / U_r h \tan\varepsilon$
h	= lobe height at 60 mm
I_s	= streamwise circulation $\oint U_s \, ds$, Eq. (1)
m	= mass flow-averaged total pressure loss $C_D \int U^3 \, dA$, where $C_D = 0.002$, Eq. (3)
Re	= Reynolds number, $U_r \lambda / \upsilon$
S	= shape factor, $\int \rho U \, dA_{\text{wake}} / \rho U_r A_{\text{wake}}$, Eq. (2)
U, V, W	= streamwise, horizontal, and vertical velocities
U_H, U_L	= the highest and lowest velocity within the wake
U_r	= reference mean velocity, $(U_1 + U_2)/2$
U_1, U_2	= mean velocity of the top and bottom streams
V_s	= secondary mean velocity, $\sqrt{(V^2 + W^2)}$
x, y, z	= streamwise, horizontal, and vertical directions
ε	= half of the included divergent angle of the penetration region, 22 deg
λ	= nominal lobe wavelength at 60 mm
ρ	= density
υ	= kinematic viscosity

I. Introduction

MORE than four decades have passed since forced mixers were first examined in their applications in jet exhaust systems. However, detailed laboratory experiments have only been performed in the past two decades. The use of computational fluid dynamics (CFD) in the analysis of lobed mixers is somewhat newer, at less than 10 years.

At present, the designs of mixer geometry that could yield the highest system performance are dependent on the execution of experiments to generate empirical design guidelines. At the same time, detailed benchmark experimental data are also collected for the validation of different CFD codes so that more accurate and reliable programs may be used as future design tools.

Received 24 May 1998; revision received 20 March 1999; accepted for publication 4 May 1999.

*Associate Professor, Thermal and Fluids Engineering Division, School of Mechanical and Production Engineering. Member AIAA.

†Research Student, Thermal and Fluids Engineering Division, School of Mechanical and Production Engineering.

Previous investigations on the low-bypass-ratio engine with a lobed mixer showed that the rapid mixing of the core and the bypass flows induced by the convoluted trailing-edge geometry could effectively reduce the jet noise and enhance the thrust.[1,2] Some improvements could also be gained by specific fuel consumption.[3]

It is well recognized that the effectiveness of a lobed mixer should be largely determined by the strength of the streamwise circulation shed at the trailing edge.[4,5] The strength of the streamwise circulation is primarily controlled by the geometry of the trailing-edge convoluted surface.[6–10] This includes the trailing-edge profile, the lobe penetration angle, and lobe ramp shape. The flow conditions (e.g., velocity ratios or the upstream boundary-layer thicknesses) may also have an effect on the strength of the streamwise circulation generated.[9,11] A good summary of the investigations of lobed mixer flow at low speeds can be found in Waitz et al.[12]

Lobes of straight parallel sidewalls were far superior to those of other geometries, in terms of maximizing the strength of streamwise circulation at the trailing edge. Based on the prediction of inviscid flow theory[5] and, ideally, to maximize the strength of the streamwise circulation, the penetration angle should be as large as possible. Massive flow separation, however, would appear if the penetration angle were above 22 deg (for the case of low Mach number flows), which in turn would induce a substantial loss to the streamwise-circulation strength.[9,11] The penetration angle may increase beyond 22 to ~35 deg by use of the scalloped lobes (i.e., by partial removal of the sidewall of the straight sections). Presz et al.[3] showed that using the scalloped lobes in a lobed mixer of aggressive penetration angles could reduce the likelihood of boundary-layer separation. In the application of an ejector, the scalloped mixer can produce a pumping performance that approaches ideal values. The investigation of Presz et al.[3] also suggested that additional streamwise vortices would be formed as a result of the scalloping, and thereby enhance the mixing. This was further confirmed in the experiments conducted by Yu et al.[13] Scalloping the lobes could enhance the streamwise circulation by ~30%, comparing with the streamwise circulation of a normal lobed mixer with the same penetration angle and trailing-edge profile. Apart from scalloping the lobes, scarfing the lobes would also enhance the strength of the trailing-edge streamwise circulation. In the laser Doppler velocity measurements of Koutmos and McGuirk,[14] a scarfed mixer was shown to generate a streamwise circulation 25–30% stronger than that generated by the normal lobed mixer.

It is thus obvious that both scarfing and scalloping the lobes would enhance the strength of the streamwise circulation. It is therefore worthwhile to conduct a detailed comparative study on these two types of mixers so as to determine the corresponding benefits arising from either modification. Furthermore, scalloped mixers have already received some attention in the past, but the detailed flow characteristics of the scarfed mixer have yet to be determined. In this paper, a systematic investigation of the scalloped mixer and scarfed mixer is summarized. In addition, their combined effects, that is, a so-called scarfed and scalloped mixer, is also discussed.

Although this investigation is limited to low-speed flow, the detailed measurements would be useful for the validation of different CFD codes. Furthermore, based on the investigations of Barber et al.,[5] the generation of streamwise vorticity by a lobed mixer is basically an inviscid process. Some similarities in the flow behavior in the vicinity of the mixer trailing edge would therefore be expected when the mixers considered here are applied to high-speed flow situations.

Section II briefly describes the experimental setup for velocity measurement purposes, including the three-hole pressure probe and the laser Doppler anemometer. Section III gives a presentation and discussion of the results. Section IV concludes the paper with a summary of more important findings.

II. Flow Configurations and Instrumentation

A. Wind Tunnel

The wind tunnel used for velocity measurements in this investigation was an open circuit, suction type that had a contraction-to-area ratio of 10:1. This large contraction ratio ensured a uniform core flow and a relatively low turbulence level (<1% of the inlet bulk velocity) on entry to the test section. The Plexiglas test section is 200 mm high, 200 mm wide, and 500 mm long. The model lobed mixer was mounted at the entrance to the test section at a central position so that on either side of the splitter plate there was the same area of flow. Different velocity ratios between the upper and lower streams were achieved by incorporating screens and wire meshes on one side of the lobed mixer. The speed range of the wind tunnel, in the absence of the lobed mixer, was from 5 to 25 m/s (maximum Mach number of ~0.07). In this paper, the results for a mean speed of 8 m/s are presented, which correspond to a Reynolds number of 3.28×10^4 (based on the nominal wavelength of the lobe at 60 mm). Further details of the wind tunnel can be found in Ref. 15.

Velocity measurements were obtained with a three-hole pressure probe and a two-component laser Doppler anemometer. The former was used to evaluate the streamwise-circulation strength at respective downstream stations behind the trailing edge (see Fig. 1), whereas the latter was used for velocity measurements across an entire cross-sectional plane of interest.

B. Lobed Mixer Configurations

The lobed mixers were made of 1.5-mm-thick fiberglass with a blunt trailing edge. Each mixer had six lobes with a nominal wavelength of 60 mm and an included divergence angle of 44 deg. Four different types of lobed mixers were tested: the baseline lobed mixer (LM), the scalloped mixer (SM), the scarfed mixer (ScM), and the scalloped and scarfed mixer (SSM). Detailed dimensions of respective mixers and the coordinate system adopted in this experiment are shown in Figs. 2a–2d.

For the ScM and SM, a systematic comparison was also conducted to examine the effects of area changes caused by scalloping and scarfing in the penetration region on the strength of the trailing-edge streamwise circulation. The scalloped mixer is basically a lobed mixer with a certain percentage of its sidewall area removed in the penetration region. Consider the side view of a lobed mixer in Fig. 2a, which shows the penetration region. If the total area is 1, the cutoff area will be expressed as a percentage of 1, as Fig. 2b shows. Similarly, for the scarfed mixer in Fig. 2c, the area was formed by extending and cutting back on the lobes at the trailing edge. The extension begins at the trailing edge and is expressed in terms of the total area of the penetration region of a lobed mixer. The cutting back is based on the same definition. It should be noted that the amount of extension is the same as the cutoff for any particular case considered. Figures 3a and 3b show further details of these two types of mixers.

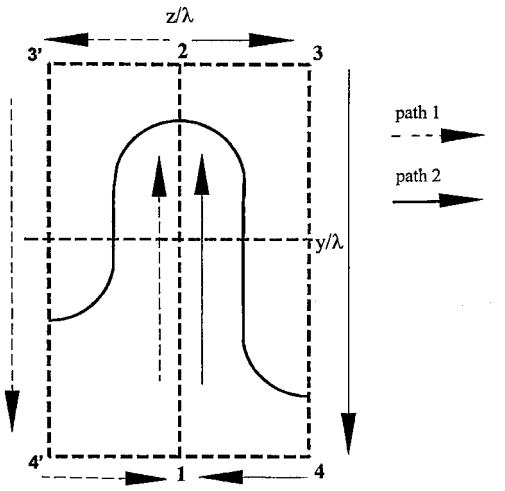

$$\Gamma_s = \oint_{1\text{–}2} \vec{W} ds + \oint_{2\text{–}3} \vec{V} ds + \oint_{3\text{–}4} \vec{W} ds + \oint_{4\text{–}1} \vec{V} ds \quad \text{(Path 1=Symmetric lobes)}$$

$$\Gamma_s = \oint_{1\text{–}2} \vec{W} ds + \oint_{2\text{–}3'} \vec{V} ds + \oint_{3'\text{–}4'} \vec{W} ds + \oint_{4'\text{–}1} \vec{V} ds \quad \text{(Path 2=Asymmetric lobes)}$$

Fig. 1 Integration path for the streamwise circulation.

C. Laser Doppler Anemometer

A four beam, two component, fiber-optic laser Doppler anemometer (manufactured by TSI Inc.) together with a 2-W argon-ion laser operating in a backward scatter mode were used to measure respective velocity components. A focusing lens of 400 mm provided a measuring probe volume of $0.09 \times 0.09 \times 1.31$ mm in the vertical direction and $0.085 \times 0.085 \times 1.24$ mm in the horizontal direction. The fiber-optic probe was mounted on an automated three-dimensional traversing system with an accuracy of ±0.01 mm. Bragg shifting of the frequency up to 2 MHz (on each channel) was used to avoid directional ambiguity. The Doppler signals were detected by photomultipliers and processed by automatic burst correlators (TSI IFA 750). Fine water particles with sizes of 5–10 μm that were generated by a commercial vaporizer were used to seed the flow. They were injected into the wind tunnel upstream of the settling chamber before the contraction section. Except at some regions immediately behind the trailing edge, data rates of 500–1000 Hz were normally obtainable. At each measuring point, the mean velocities (U and V), the rms of the velocity fluctuations (u' and v'), and the Reynolds shear stresses ($\overline{u'v'}$) were determined from populations of more than 5000 (on each channel) samples together with a coincidence window of 1 μs. The W components were obtained by rotating the fiber-optic probe by 90 deg with respect to the test section. The temperature of the air was kept at 28° during the course of the experiment.

The possible sources of uncertainty associated with the measurements of velocity were considered in detail by Hou[15] and include aspects of optical arrangements, the signal- and data-processing systems. In short, the maximum uncertainties in the ensemble-averaged mean and rms velocities are of 1 and 2% (normalized by U_r), respectively. All the above-mentioned sources were estimated based on a 95% confidence level.

Measurements of the three orthogonal mean velocities (U, V, W) and their corresponding rms fluctuations (u', v', w') were acquired in the projected area corresponding to the one full lobe, and at downstream locations $x/\lambda = 0.25$, 0.5, 1, 2, 3, 4, 5, and 6. There were ~1100 measuring points at each plane presented here. Velocity

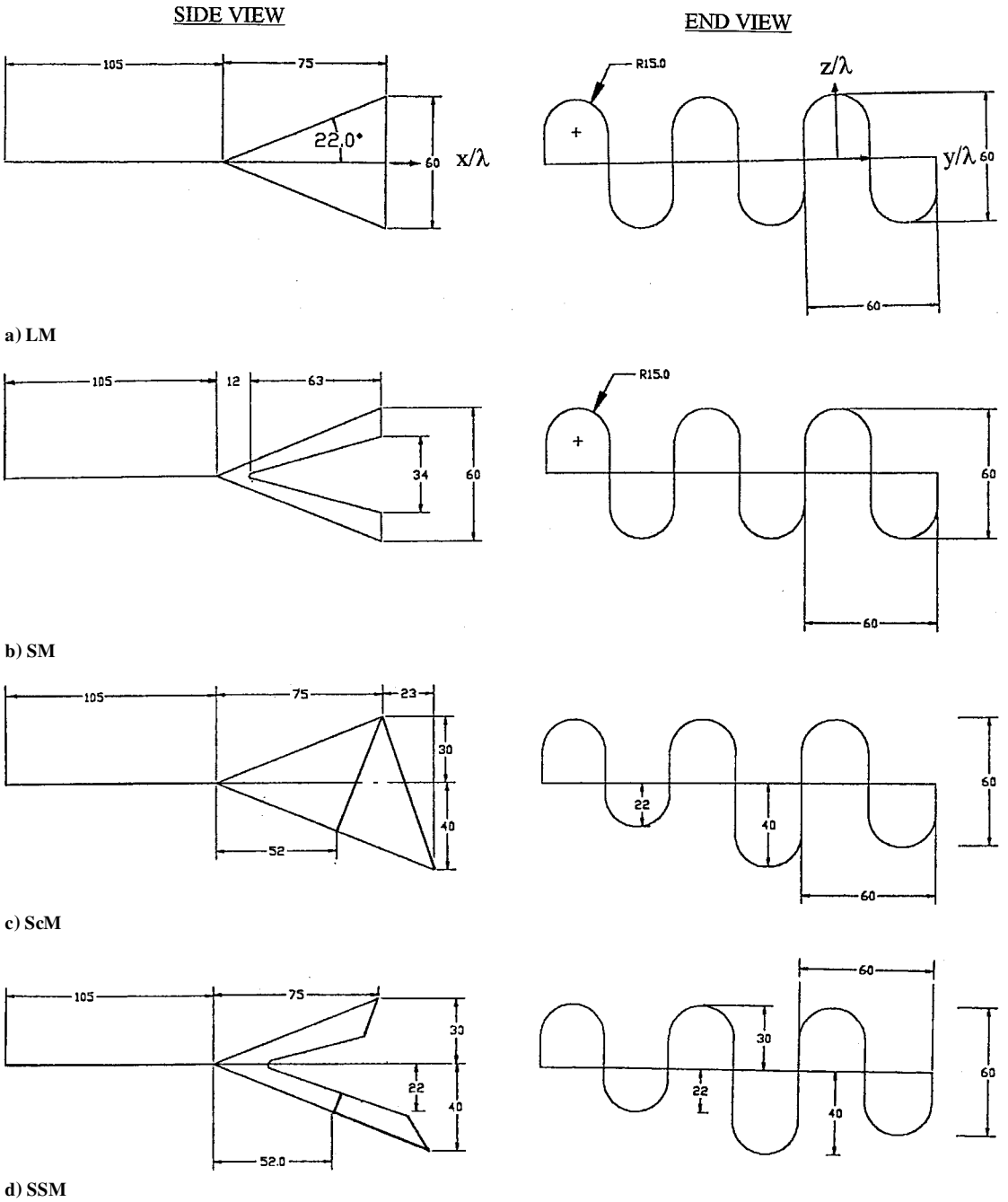

Fig. 2 Mixer geometries under investigation (all dimensions are in mm).

measurements were also obtained along the circulation paths (see Fig. 1) with a calibrated three-hole pressure probe with a nominal probe tip size of 3 mm at locations $x/\lambda = 0.5$, 1, 2, 3, 4, 5, and 6. The pressure output was connected to an inclined manometer with a resolution of ±0.005 kPa.

Three velocity ratios, 1.0, 0.5, and 0.3, across each lobed mixer were tested. At each velocity ratio, three different thicknesses of the initial boundary layer (measured at three wavelengths upstream of the penetration region) were used, and they corresponded to $\frac{1}{2}$, $\frac{1}{3}$, and $\frac{1}{10}$ of the trailing-edge wavelength.

III. Results and Discussion

A. General Features of the Flowfield near the Trailing Edge

1. Lobed Mixer, Scalloped Mixer, and Scarfed Mixer

Contours of the measured normalized streamwise mean velocities and the corresponding secondary flow velocity vectors for respective mixers at velocity ratios of 0.5 and $x/\lambda = 0.5$ are shown in Figs. 4a–4c. Further details of the results can be readily found in Ref. 15.

The distribution of the contours at this station provided some good indications for the effects of the streamwise vorticity on the interaction of the two coflowing streams. As may have been expected, for the baseline configuration, LM in Fig. 4a, the wake shed followed closely to the projected shape of the lobe trailing-edge profile. For the SM (with a 30% sidewall area removal) in Fig. 4b, a pair of streamwise vortices was generated within a half-lobe. Although the two vortices had their origins from opposite streams,[13] they were actually rotating in the same sense (counterclockwise direction) and thus greatly enhanced the transportation of the fluids across the lobe. Two vortices of relatively smaller size but of higher strength can facilitate mixing between the two coflowing streams at a finer scale and faster rate. A further increase in the scalloping effects would enhance the strength and size of the two vortices. For the scarfed mixer in Fig. 4c (ScM with a 30% area change), a pair of asymmetric streamwise vortices were formed at the wake and their cores were at a region closer to the lobe troughs. As a result of the extending and cutting back of the lobes, the wake shed did not follow closely to the shape of the trailing-edge profile; this observation is similar to that

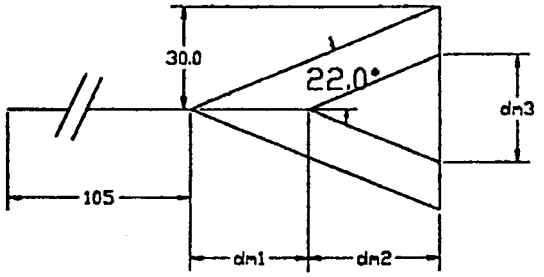

(%)	dm1	dm2	dm3
10	62	13	14
20	41.5	33.5	27
30	35	40	34
40	27.5	47.5	38
50	21	54	43
60	17	58	47
70	12	63	51
80	8	67	54

a) SM

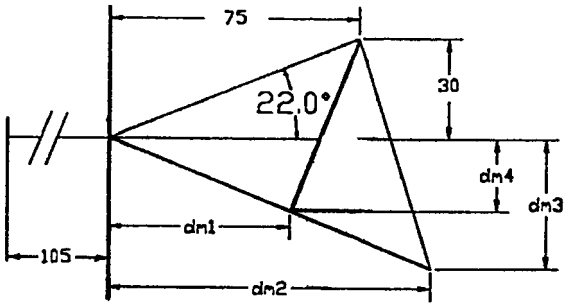

(%)	dm1	dm2	dm3	dm4	dm5	dm6	dm7	dm8	dm9
10	67.5	82.5	33	27	82.5	67.5	7	33	27
20	60.6	89.6	36	24	89.6	60.8	7	36	24
30	54.5	96	39	21	96	54.4	7	39	21
40	49.5	103	42	18	103	50	7	42	18

b) ScM

Fig. 3 Dimensions of the scalloped mixer and the scarfed mixer at different percentages of area change at the penetration region (all dimensions are in mm).

for the scalloped mixer. The vortex generated within the short gulley appeared to have a higher strength of secondary flow. When the lower stream had a higher speed, two streamwise vortices also were formed, but the locations of their cores were closer to the peak of the lobes (results not shown here). Again, the strength of the vortex generated within the short gulley was relatively higher.

Based on the velocity measurements at successive downstream stations, for the flow conditions shown in Figs. 4b and 4c, schematic views of the flow structure in the vicinity of the trailing edge for the SM and ScM can be constructed. As shown in Fig. 5b for the ScM, the formation of the streamwise vortices was different within the short and long gulleys. Within the short gulley an observation similar to that for the SM in Fig. 5a was found, in which the interaction of the two fluid streams was greatly facilitated by the cutting back of the trailing edge. The rolled-up configuration of the streamwise vortices is reminiscent of the flows behind a delta wing. The flows in the vicinity of the short gulley essentially had the same effects as the scalloped mixer. However, within the long gulley, the formation mechanism of the streamwise vortex was the same as the normal lobed mixer. Largely because of the extension of the trailing edge, the two streams did not fully interact until they were at $\sim x/\lambda = 1.5$. Despite this, as shown later (in Fig. 9), this delay does not cause the wake flow to achieve spatial uniformity at a longer downstream distance that is longer than that of the LM and SM. It should also be noted that the axes of the streamwise vortices may not be parallel to the streamwise direction but are tilted at an angle relative to the streamwise direction. This may explain in part why the scarfed mixer can actually provide a more efficient momentum transfer across the two streams.

2. *Scarfed and Scalloped Mixer*

Of particular note is that only a minor improvement, in terms of trailing-edge streamwise-circulation strength, could be achieved by scalloping the scarfed mixer (~5% and mainly within the long gulley). As shown in the contour plots of Fig. 6, where the upper stream had a higher velocity, the pair of streamwise vortices formed in the wake were further strengthened by the effects of scalloping. The wake shed was also found to be slightly more diffused than that without scalloping in Fig. 4c, especially in the region close to the lobe troughs. However, when the lower stream had a higher speed (not shown here), the strength of the streamwise vorticity remained at the same order of magnitude compared with that without scalloping (i.e., similar to that of the ScM). It is thus obvious that scalloping the scarfed mixer would only be beneficial in situations in which the high-speed stream is along the long gulley.

B. Variation of the Streamwise Circulation with Downstream Distance

The strength of the streamwise vorticity at different downstream locations may be quantified by evaluation of the streamwise circulation along a rectangular path that encompasses one-half the lobe wavelength, as shown in Fig. 1. In a nondimensional expression,[5]

$$C_1 = \frac{\Gamma_s}{U_r h \tan \varepsilon} \tag{1}$$

where

$$\Gamma_s = \oint_{1-2} \boldsymbol{W}\,\mathrm{d}s + \oint_{2-3} \boldsymbol{V}\,\mathrm{d}s + \oint_{3-4} \boldsymbol{W}\,\mathrm{d}s + \oint_{4-1} \boldsymbol{V}\,\mathrm{d}s$$

for symmetric lobes (path 1) and

$$\Gamma_s = \oint_{1-2} \boldsymbol{W}\,\mathrm{d}s + \oint_{2-3'} \boldsymbol{V}\,\mathrm{d}s + \oint_{3'-4'} \boldsymbol{W}\,\mathrm{d}s + \oint_{4'-1} \boldsymbol{V}\,\mathrm{d}s$$

for asymmetric lobes (path 2).

With the exception of the LM and the SM, other configurations were not symmetrical at every half-lobe. For these cases, the values for the two circulation paths is also considered.

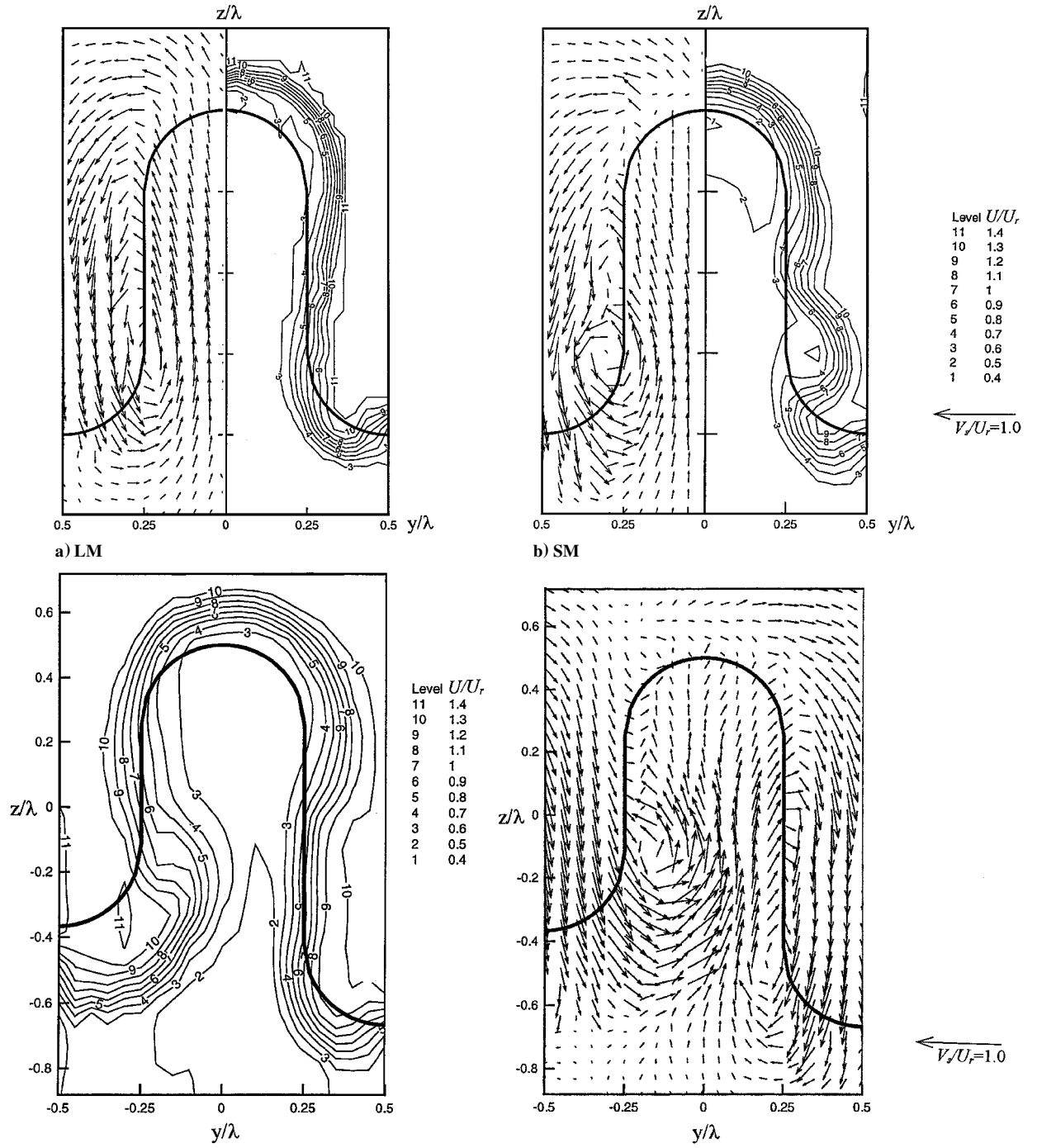

Fig. 4 Contours of the measured normalized streamwise mean velocity (U/U_r) and the corresponding secondary flow velocity vectors (V_s/U_r) at $x/\lambda = 0.5$ for respective mixers.

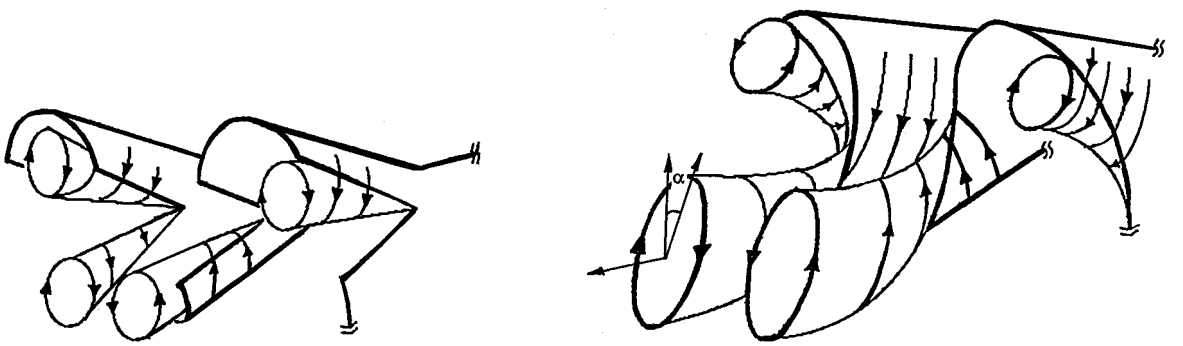

a) All the vortices lie on the same plane, parallel to the trailing edge

b) All the vortices do not lie on the same plane, parallel to the trailing edge

Fig. 5 Schematic of the flow structure in the vicinity of the a) SM and b) ScM trailing edge.

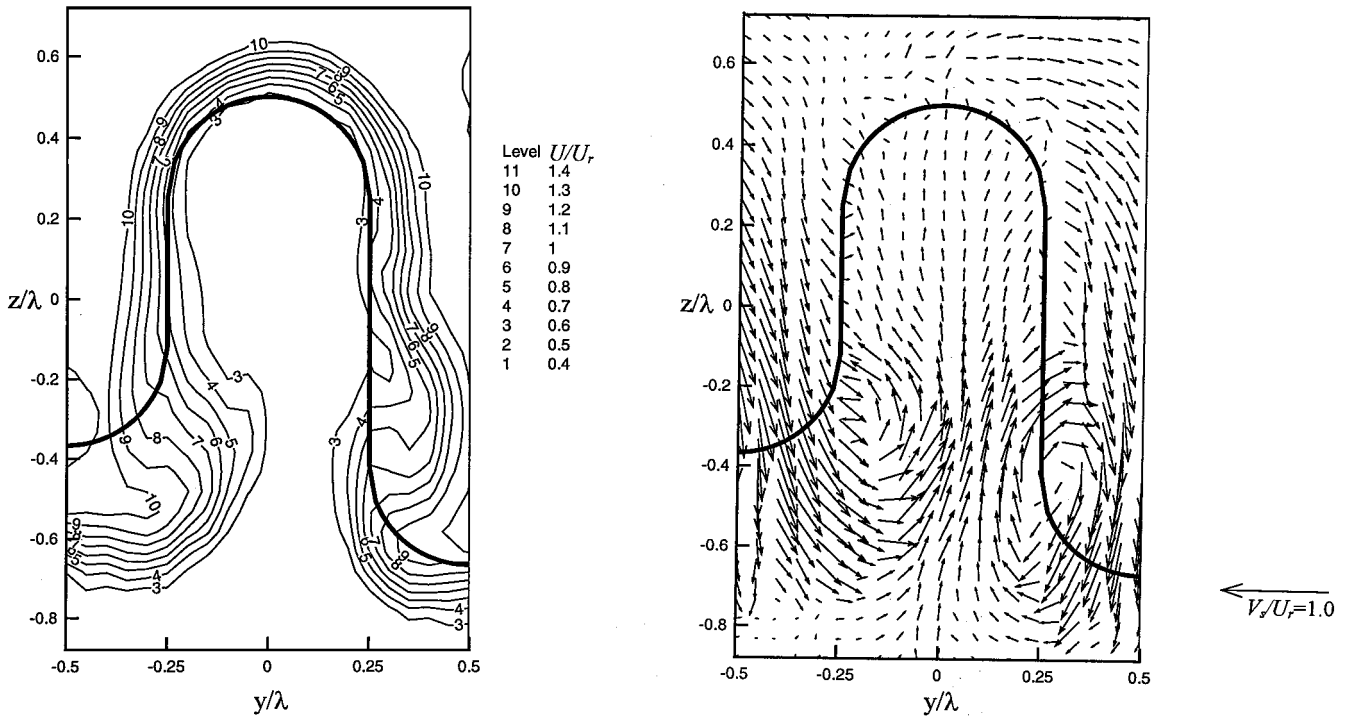

Fig. 6 Contours of the measured normalized streamwise mean velocity (U/U_r) and the corresponding secondary flow velocity vectors (V_s/U_r) at $x/\lambda = 0.5$ for the SSM.

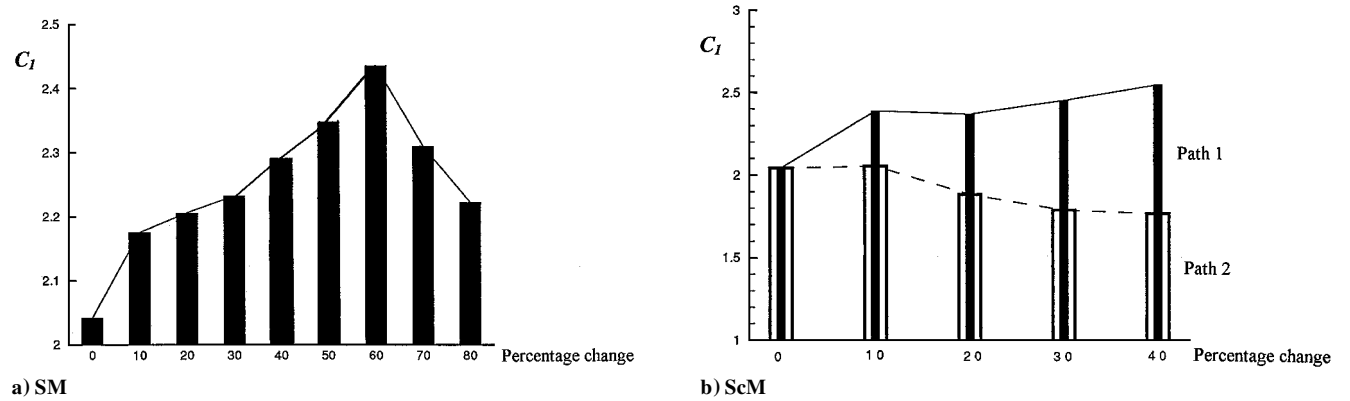

Fig. 7 Effects of area change at the penetration region for the SM and the ScM.

1. Effects of Area Changes at the Penetration Region

Figures 7a and 7b show the streamwise-circulation values for the SM and ScM at different percentages of area change at the penetration region at $x/\lambda = 0.5$ when the velocity ratio was 0.5. Several important conclusions can be drawn from Fig. 7. A maximum increase of ~25% in strength can be achieved by scalloping up to 60% of the sidewall area. After this, the increasing trend ceases. Similarly, a maximum increase of ~30% in strength can also be achieved at the long gulley by scarfing the lobes to ~40%. It was surprising to see that the streamwise-circulation strength within the long gulley stayed nearly at the same level as the area change increased. Further experiments were not conducted for the scarfed mixer of more than 50% area change because of excessive cutting of the area at the short gulley, which in turn weakened the structural support of the lobe. Thus, given the same percentage of area change (see, e.g., the 40% case), the enhancement in streamwise circulation for the scarfed case within the short gulley was some 15% higher than that for the scalloped case.

2. Variation of Streamwise Circulation with Downstream Distance

The decay of the streamwise circulation for the ScM and SSM at a velocity ratio of 0.5 is shown in Figs. 8a and 8b. Some general characteristics are summarized here. For the ScM in Fig. 8a, the distance required for the streamwise circulation to decay completely was ~4λ, for the streamwise circulation values at both the long and short gulleys. For the SSM in Fig. 8b, the decay length was found to be longer (at ~6λ). Although the strength of the streamwise circulation for this case had the highest value at the trailing edge, the decay length was also the longest.

The decay of the streamwise circulation is largely affected by two factors: viscosity and diffusion of streamwise vorticity. The latter is also closely associated with the interaction between two neighboring vortices within a lobe (which may enhance or suppress the strength of the streamwise vortices). Because the two neighboring vortices within a lobe for the ScM and SSM were of opposite sign, it was very likely that the strength of the streamwise circulation would be suppressed when they interacted. As already shown in the trailing-edge circulation values for the ScM, the streamwise vortex generated within the short gulley was stronger than that generated within the long gulley, but it was weaker than that generated by the SSM mixer. The two neighboring vortices began to interact with each other at approximately the same streamwise location, that is, at approximately 2–3λ from the trailing edge. The overall circulation for the SSM remained higher than that of the ScM, because of a stronger vortex generated at the short gulley and because for both the

ScM and SSM the streamwise circulations within the long gulley had nearly the same strength. This may partially explain the difference in the distance of decay for the SSM and ScM in Figs. 8a and 8b.

It should be noted that, at this velocity ratio, the decay rate for the LM was independent of the thicknesses of the initial boundary layers, as may have been expected.[11] The maximum decay distance was $\sim 4\lambda$. For the SM the decay was also independent of the initial boundary-layer thicknesses, but the decay distance was shorter than that of LM, at $\sim 3\lambda$.

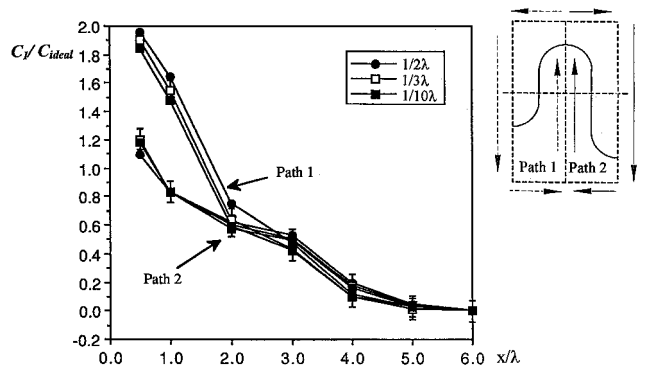

a) ScM

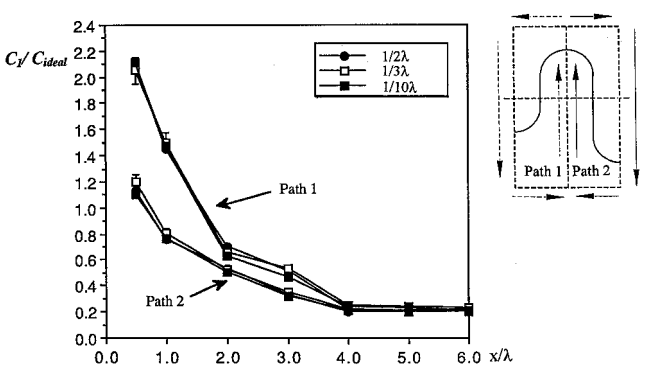

b) SSM

Fig. 8 Variation of the normalized streamwise circulation with downstream distance (the results are normalized by the theoretical value obtained by the analysis of Ref. 5).

C. Spatial Uniformity with Downstream Distance

The variations of the spatial uniformity with downstream distance are shown in Fig. 9 for various cases. The mixing of the two flows within the wake region in terms of mass flux distribution is of interest. Therefore, it may be sufficient to define the mixing-level parameter for the two streams in terms of the shape factor of the streamwise mean velocity distribution:

$$S = \frac{\int \rho U \, dA_{\text{wake}}}{\rho U_r A_{\text{wake}}} \tag{2}$$

Integration of the mass flux was performed on either side of the lobed mixers (i.e., the high- and low-speed sides, respectively). Ideally, at the location where the two streams at the wake region with different velocities is to be completely mixed and spatial uniformity could be achieved, the mass flux distribution would be uniform and the shape factor should be equal to one. The variation of the shape factor as a function of downstream distance should provide a useful indication of the extent of the spatial uniformity that the two flows can achieve.

As shown in the Fig. 9, the SM could actually achieve the fastest spatial uniformity at the shortest distance from the trailing edge ($\sim 4\lambda$), and it was followed by the ScM ($\sim 4.5\lambda$), SSM ($\sim 5\lambda$) and LM ($\sim 5\lambda$). It was also interesting to see that the ScM can also achieve uniformity at a rate similar to that of the SM and LM despite the extension of the long gulley. It may not be too surprising to see that the LM has the slowest rate among the four cases if one considers that the LM actually had the lowest strength of streamwise circulation at the trailing edge.

D. Estimation of Losses from Scalloping and Scarfing

Because the generation of streamwise circulation by respective mixers is largely responsible for the mixing augmentation, it is important to quantify the penalties (or losses) associated with the generation of the streamwise circulation. The total losses that occur in lobed mixer configurations can be divided into mixing and boundary-layer losses,[9,16] Mixing losses contain contributions from the mixing out of nonuniformities associated with the velocity field's exiting the lobes, whereas boundary-layer losses are caused by the wetted surfaces.

An analysis similar to that of O'Sullivan et al.[9] is used here. A constant area mixing process was employed to calculate the fully mixed-out loss. The flowfield nearest the trailing edge was used as inflow conditions to a control volume and then mixed out to a

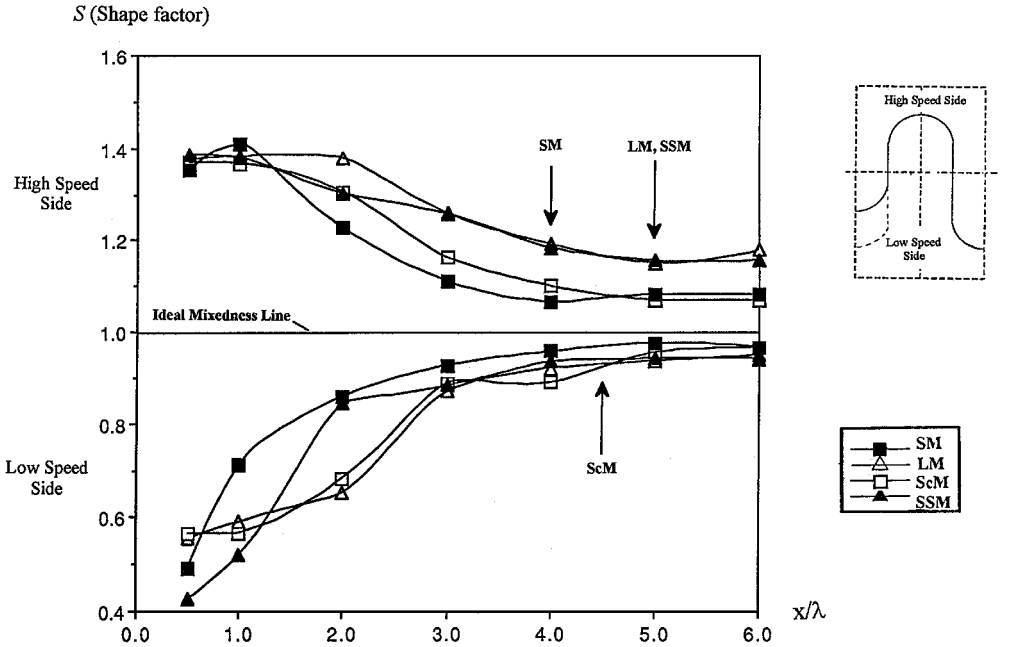

Fig. 9 Variation of the shape factor with downstream distance for respective mixers (estimated locations for complete mixing are indicated by arrows).

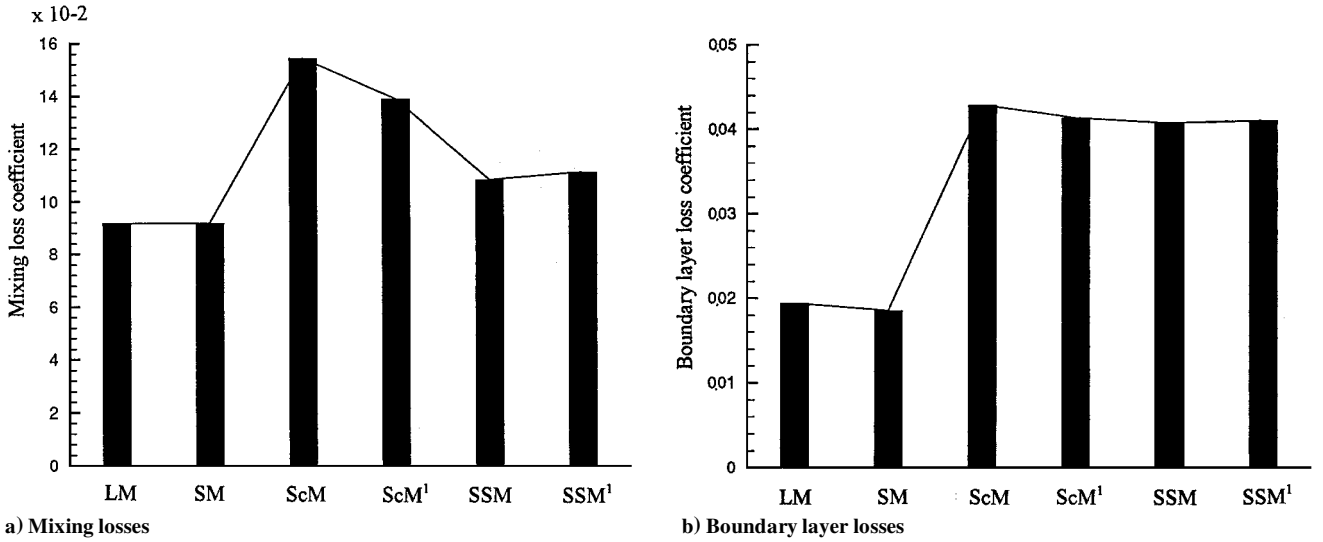

Fig. 10 Estimation of mixing and boundary-layer losses for respective mixers. (Superscript 1 represents high speed flow at the lower stream.)

uniform flow. The boundary-layer losses were estimated by using an empirical relationship by Cumpsty,[16] which relates the entropy production in the boundary layer to the integral of the cube of the local free-stream velocity:

$$\text{Mass flow-averaged total pressure loss}\,(m) = C_D \int U^3 \,\mathrm{d}A \quad (3)$$

C_D is not a strong function of Reynolds number for turbulent boundary layers. A value of 0.002 was used.[9,15] For the constant total temperature mixing process, Eq. (3) can be used to examine the change of total pressure.

Results for the mixing losses that contain contributions from the mixing out of nonuniformities associated with the velocity field's exiting the lobes (at $x/\lambda = 0.5$) are shown in Fig. 10a for respective mixers at a velocity ratio of 0.5. The LM and the SM were of similar values. The ScM was ~50% higher and could be attributed to the existence of the long gulley, which enabled the further growth of the boundary layers at the penetration region. Results for the SSM lay in between the LM (and SM) and ScM cases.

Boundary-layer losses caused by the wetted surfaces were considered on the lobe surfaces, the lower and the upper walls of the tunnel. The results are shown in Fig. 10b. The losses on the lower and upper walls were generally very much lower compared with those within the lobe. It appears that rapid mixing was confined within the wake behind the lobes. The flows along the top and bottom walls were not greatly affected. However, the effects would be more significant if the distance between the top and bottom walls was small. As pointed out in the studies of O'Sullivan et al.[9] (where the distance between the walls was 2λ compared with $\sim 7\lambda$ here), the losses on the walls could be as high as 20 times those found in the lobes. For the velocity ratio of 0.5 investigated here, mixing losses accounted for more than 90% of the total loss. For typical velocity ratios encountered in practice (>0.5), mixing losses downstream of the lobe trailing edge will typically be the largest contribution to the total loss incurred.

IV. Conclusions

This paper summarized the major findings on two important aspects of geometric modifications to a lobed forced mixer, namely scarfing and scalloping. Scarfing the lobes was achieved by alternately extending and cutting back the lobes at the trailing edge, and scalloping the lobes was achieved by removing a certain percentage of the straight sidewall area in the penetration region.

Tests were conducted over a range of low-speed subsonic flow conditions by using a three-hole pressure probe and a laser Doppler anemometer. The following conclusions can be drawn from the preceding text. First, for the same level of enhancement to be achieved for the streamwise circulation, scarfing the lobes required a smaller percentage of surface area change at the penetration region than scalloping the lobes. Furthermore, streamwise circulation generated at the trailing edge was actually higher (maximum at ~15% for a 40% area change) by scarfing of the lobes than by scalloping of the lobes if both had the same surface area change at the penetration region. Second, the combined effects of both modifications on a lobed mixer, that is, a scarfed and scalloped mixer, could increase the streamwise circulation at the trailing edge by approximately 5–10%, but the subsequent decaying distance was much longer than that of the other cases considered here. Third, within the range of flow conditions tested, scalloped lobes showed the fastest decay rate for the streamwise vorticity and the shortest distance to attain mass flux uniformity at the wake. It was followed by the scarfed mixer, the scarfed and scalloped mixer, and finally by the lobed mixer. Fourth, an estimation of the mixing and boundary-layer losses showed that with the exception of the lobed mixer, the scalloped mixer can also provide lower losses compared with the other configurations. This may be because the scalloped mixer has the lowest surface contact area (wetted surfaces) within the penetration region.

Acknowledgments

Financial support for this project from the Academic Research Fund and the contributions of C. T. Quek and A. Tan for the velocity measurements are gratefully acknowledged.

References

[1] Presz, W. M., Blinn, R. F., and Morin, B., "Short Efficient Ejector Systems," AIAA Paper 87-1837, Jan. 1987.

[2] Presz, W. M., Gousy, R., and Morin, B., "Forced Mixer Lobes in Ejector Design," *Journal of Propulsion and Power*, Vol. 4, No. 4, 1988, pp. 350–360.

[3] Presz, W. M., Reynolds, G., and McCormick, D., "Thrust Augmentation Using Mixer-Ejector-Diffuser Systems," AIAA Paper 94-0020, Jan. 1994.

[4] Paterson, R. W., "Turbofan Mixer Nozzle Flowfield—A Benchmark Experimental Study," *ASME Journal of Engineering for Gas Turbines and Powers*, Vol. 106, 1984, pp. 692–698.

[5] Barber, T., Paterson, R. W., and Skeba, S. A., "Experimental Investigation of Three-Dimensional Forced Mixer Lobe Flow Fields," AIAA Paper 88-3785, Jan. 1988.

[6] Eckerle, W. A., Sheibani, H., and Awad, J., "Experimental Measurement of the Vortex Development Downstream of a Lobed Forced Mixer," *ASME Journal of Engineering for Gas Turbines and Power*, Vol. 114, 1992, pp. 63–71.

[7] McCormick, D. C., and Bennett, J. C., Jr., "Vortical and Turbulent Structure of a Lobed Forced Mixer Free-Shear Layer," *AIAA Journal*, Vol. 32, No. 9, 1994, pp. 1852–1859.

[8] Yu, S. C. M., and Yip, T. H., "Measurements of Velocities in the Near Field of a Lobed Forced Mixer Trailing Edge," *The Aeronautical Journal of the Royal Aeronautical Society*, Vol. 101, March 1997, pp. 121–129.

[9]O'Sullivan, M. N., Waitz, I. A., Greitzer, E. M., Tan, C. S., and Dawes, W. N., "A Computational Study of Viscous Effects on Lobed Mixer Flow Features and Performance," *Journal of Propulsion and Power*, Vol. 12, No. 3, 1996, pp. 449–456.

[10]Manning, T. A., "Experimental Studies of Mixing Flows with Streamwise Vorticity," M.S. Thesis, Gas Turbine Lab., Massachusetts Inst. of Technology, Cambridge, MA, Sept. 1991.

[11]Yu, S. C. M., Xu, X. G., and Yip, T. H., "The Effects of Initial Boundary Layer Thicknesses to the Trailing Streamwise Vorticity in a Lobed Forced Mixer," *Journal of Propulsion and Power*, Vol. 14, No. 2, 1996, pp. 440–442.

[12]Waitz, I. A., Qiu, Y. J., Manning, T. A., Fung, A. K. S., Elliot, J. K., Kerwin, J. M., Krasnodebske, J. K., O'Sullivan, M. N., Tew, D. E., Greitzer, E. M., Marble, F. E., Tan, C. S., and Tillman, T. G., "Enhanced Mixing with Streamwise Vorticity," *Progress in Aerospace Science*, Vol. 33, 1997, pp. 323–351.

[13]Yu, S. C. M., Yip, T. H., and Liu, C. Y., "The Mixing Characteristics of Forced Mixers with Scalloped Lobes," *Journal of Propulsion and Power*, Vol. 13, No. 2, 1997, pp. 305–311.

[14]Koutmos, P., and McGuirk, J. J., "Velocity and Turbulence Characteristics of Isothermal Lobed Mixer Flows," *ASME Journal of Fluids Engineering*, Vol. 117, No. 4, 1995, pp. 633–638.

[15]Hou, Y. X., "Applications of Laser Doppler Anemometry (LDA) to the Study of Some Industrial Two-Stream Mixing Flow Processes with Streamwise Vorticity," MEng. Thesis, School of Mechanical and Production Engineering, Nanyang Technological Univ., Singapore, 1999.

[16]Cumpsty, N. A., *Compressor Aerodynamics*, Longman Group, Essex, England, UK, 1989.